

Stress shielding reduced by a silicon plate-bone interface

A canine experiment

Donna L. Korvick,¹ Jarrett W. Newbrey,² George W. Bagby,³ Ghery D. Pettit¹ and James D. Lincoln¹

Effects of modifying the plate-bone interface with Silastic[®] were tested. The experimental plate, i.e., a conventional plate with a Silastic[®] backing was compared with the standard plate. In vitro four-point bending tests showed similar strain per load behavior in the experimental and standard plate models. In vitro plate-bone contact was greater and interface pressure was lower for the experimental as compared with the standard plate. An in vivo implant study was conducted where the plates were tested on intact canine femurs. At 27 weeks postimplantation, there was less porosity and remodeling in the haversian envelope of bone plated with a Silastic[®] interface.

Plate-induced bone loss occurs late in fracture remodeling and is attributed to stiffness differences between implant and bone (Akeson et al. 1976). In vivo studies showed up to 80 percent bone strain reduction following plate application, with the greatest reduction occurring directly under the plate (Schatzker et al. 1978). Plate-related bone loss is also attributed to the plate's interference with the bone's blood supply, especially where the plate contacts the bone's surface (Gunst 1980). Ischemia and osteonecrosis are thought to induce a remodeling response that reduces bone strength. Morphologic changes following bone plating include thinning of the bone cortex and expansion of haversian canals (Uthoff et al. 1971). Mechanical tests on plated bone show reduced bone strength and energy absorption (Låftman et al. 1980). These experiments explain why the bone may refracture following bone-plate removal.

Our objectives were to determine how modifications in the plate-bone interface with a viscoelastic ma-

terial would 1) affect rigidity of the plate-bone system, 2) affect contact area and pressure of the implant-bone interface, and 3) affect bone morphology and remodeling in a chronic implantation study.

Materials and methods

Plate preparation

Six-hole or 8-hole 316-L stainless steel compression plates with oval screw holes (Howmedica) were used (dimensions: 102 x 12 x 3.8 mm and 133 x 12 x 3.8 mm, respectively). The experimental plate was prepared by cutting a template of Silastic[®] Sheeting (1.5-mm thick, Dow Corning) to match the plate's shape. The Silastic[®] was bonded to the bone plates with Type A Silastic[®] Medical Adhesive and steam sterilized (Figure 1).

Mechanical evaluation of the plates

A plate-bone model was tested under quasi-static load in four-point bending. An aluminum tube was used to model intact bone (50.8-cm length, 2.54-cm diameter, 0.76-cm wall thickness, elastic modulus 70 GPa). No axial compression was created when the plate was attached to the aluminum tube with eight 4.5-mm cortical bone screws tightened to 1.6 N-m.

Departments of Veterinary Medicine and Surgery¹ and Veterinary Comparative Anatomy, Physiology and Pharmacology² Washington State University, Pullman, WA, and Department of Orthopedics³, Sacred Heart Medical Center, Spokane, WA, USA

Correspondence: Dr. Donna Korvick, 2001 South Lincoln Avenue, Urbana, IL 61801, USA.

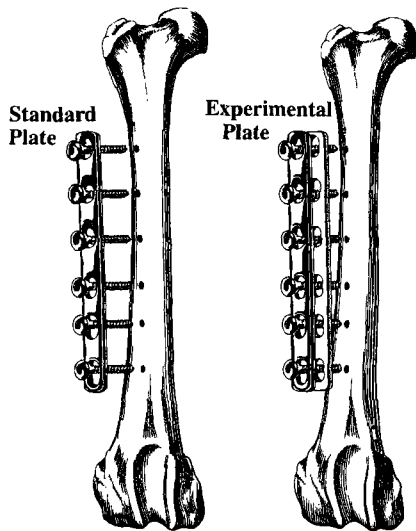


Figure 1. Standard plate and experimental plate attached to the anterolateral surface of intact femurs.

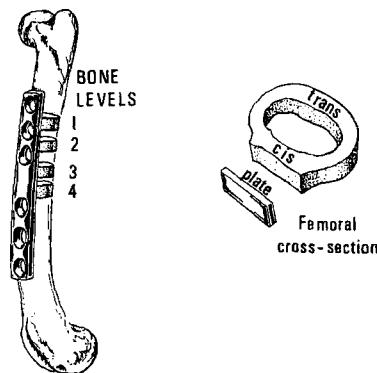


Figure 2. Location of sections used for metric and histologic analysis.

The plate and aluminum tube were instrumented with three single-element, 120 ohm, metal-foil strain gauges (Measurements Group Inc.) oriented parallel to the tube's long axis. The strain gauges were located on the midsection of the plate and tube, both under and directly opposite the plate. To accommodate the gauge under the plate, the plate was notched on the bottom surface (1.2 x 1.5 x 0.1 cm).

The model was tested in four-point closed bending on an electrohydraulic testing machine (Systems 810, MTS Corporation) and loaded from 2 to 2,200 N at the rate of 45 N/second for six repetitions. Maximum bending moment between the two inside rollers was 85 N/m. Strain gauge and applied-load readings were sampled at 1 Hz using a multichannel data acquisition system (Optilog, Optim Electronics Corporation). Least squares regression analysis showed that tube and plate strains varied linearly with load. A two-way analysis of variance was performed between standard and experimental plate slopes (μ strain/kN) and strain gauge position for six trials of each plate ($P < 0.05$).

To evaluate contact pressure and contact area between implant and bone, medium pressure sensitive Fuji prescale film (Tokyo, Japan) was used (pressure range 70 to 250 kg/cm²). Plate and film were attached to a polycarbonate tube (2.54-cm diameter, 0.32-cm wall thickness) for 2 min with six 4.5-mm cortex screws tightened to 1.6 N/m. Contact area was measured from a photographic enlargement of the Fuji film, using a digitizing pad (B & L Hipad, Houston Instruments) and an IBM-PC. Contact pressure between implant and tube was determined by visual comparison of color density with the film's standard color conversion chart. Each implant type was tested four times. One-way analysis of the variance was used to evaluate contact area ($P < 0.05$).

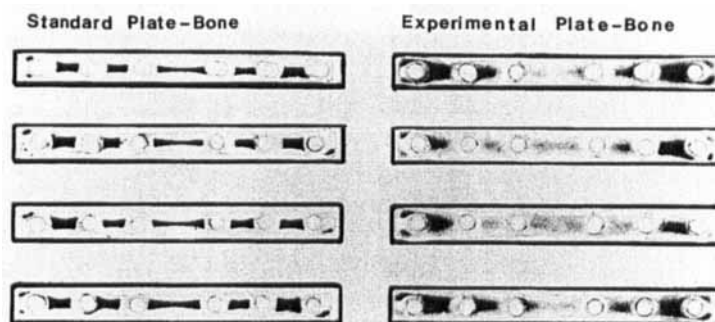
In vivo study

An *in vivo*, 27-week implant study was performed on 10 adult dogs of both sexes weighing between 20 and 30 kg. We chose a 27-week study because Uthoff (1983) has previously shown that bone loss from plate application is maximal by 24 weeks.

A six-hole standard plate was implanted on the anterolateral surface of the dog's intact femur and a six-hole experimental plate on the dog's opposite femur with 4.5-mm cortical bone screws. Following surgery the dogs received 20 mg/kg of amoxicillin per os twice daily for 5 days. All the dogs were weight bearing following surgery; however, they were confined to a cage for 1 week before being placed in outdoor runs.

To study late bone-remodeling activity, each dog re-

Figure 3. Contact area between plate and bone for the standard plate-bone and experimental plate-bone shown on Fuji prescale pressure film.



ceived 15 mg/kg body weight of tetracycline by intravenous injection 14 and 4 days prior to death. Label one was tetracycline hydrochloride (Sigma) and label two was oxytetracycline (Liquamycin[®] 100, Pfizer Inc.). Both agents were diluted in 100 ml of physiological saline solution before administration.

At 27 weeks after surgery, the dogs were killed with an overdose of pentobarbital. A sample of soft tissue covering the plate was fixed in 10 percent neutral buffered formalin, embedded in paraffin, sectioned, and stained with hematoxylin-eosin for histologic examination. The Silastic[®] sheet under the experimental plate was examined for signs of plastic deformation.

Radiographs of paired femurs were taken with screw tracts positioned perpendicular to the primary x-ray beam and evaluated for the presence of screw calus in the endosteal cortex.

Bone specimen preparation

Four cross sections were cut from the femoral diaphysis (Figure 2). Ethanol-fixed bone from levels 1 and 3 was embedded in 10 percent glycol, 90 percent methylmethacrylate (Polysciences), sectioned at 5 microns using a sliding microtome (Jung Model-K[®] American Optical Company) and stained with toluidine blue. Porosity, mean osteoid seam thickness, mean osteoid seam circumference, number of osteoid seams/mm², and resorptive cavities/mm² were measured on two bone sections per level in a 25–30 mm² area immediately under the plate. Unstained 10- μ sections were used to determine appositional rates and the percentage of fluorochrome-labeled osteons in the bone under the plates.

Measurements were made in a blind fashion using a Zeiss Mop III image analysis system (Carl Zeiss Inc., West Germany). Data analysis was based on paired *t*-testing between the experimental and standard plated bone ($P < 0.05$).

Bone from level 2 was fixed in 10 percent neutral buffered formalin, demineralized in a 25 percent formic acid with 10 percent sodium citrate solution, embedded in paraffin, sectioned, stained with hematoxylin and eosin, and examined histologically.

Bone from the fourth level was hand-ground to 75 microns thick, and microradiographs were taken using a Faxitron (Hewlett-Packard; Conlogue et al. 1987). Porosity measurements of the cortex under the plate (cis-cortex) and the cortex opposite the plate (trans-cortex) were made using the Zeiss system. Porosity was defined as the ratio of haversian and resorption canals (empty space) to total bone area. Porosity evaluation was by a two-way analysis of variance grouping location (cis versus trans) and implant type ($P < 0.05$).

Bone cross sections from the third and fourth levels were photographed. Cis- and trans-cortical thickness, medullary canal area, and bone area were measured using the Zeiss system. A paired *t*-test between implant types was performed ($P < 0.05$).

Results

Mechanical evaluation of the plate

Four-point bending tests showed no differences in strain/load between standard and experimental plates at the three strain gauge sites. The strain per load averaged 389- μ strain/kN on the cis-cortex, 434- μ strain/kN on the trans-cortex, and 36- μ strain/kN on the plate. Plate-bone interface tests showed that the silicone elastomer increased the contact area from 105 mm² for the standard plate to 231 mm². Contact pressure decreased from 225–250 kg/cm² for the standard plate to 120–140 kg/cm² at the middle and 175–225 kg/cm² at the ends of the experimental plate (Figure 3).

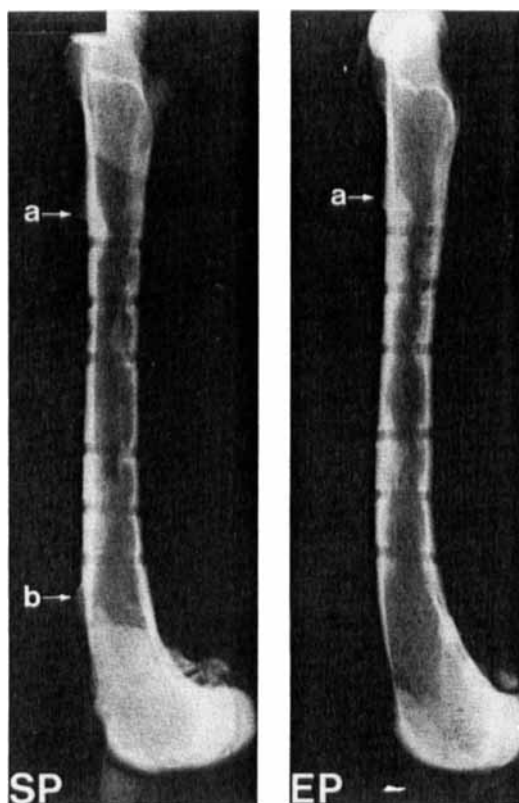


Figure 4. Radiograph of paired femurs 27 weeks after plating with the standard plate (SP) and experimental plate (EP). Note bone overgrowth at (a) the proximal plate edge and (b) the distal plate edge. Differences in distribution of callus around screw tracts can be seen.

In vivo tests

At 27 weeks, the implants were covered by a layer of dense irregular connective tissue with occasional mononuclear cells. Bone overgrew the proximal plate edge in nine of the 10 experimental and nine of 10 standard plated femurs. Bone overgrowth at the distal plate edge occurred in four of 10 standard and two of 10 experimental plated bones.

In eight of 10 experimental plates, the silicone elastomer was torn longitudinally between adjacent screw holes, but was still located between the plate and bone. Lateral displacement of the silicone elastomer did not exceed 3 mm. Connective tissue filled the 1–2-mm gap in the Silastic®.

Screw callus was evenly distributed among the six screw tracts in the experimental plated bone, but located at the proximal and distal screw tracts in standard plated bone (Figure 4).

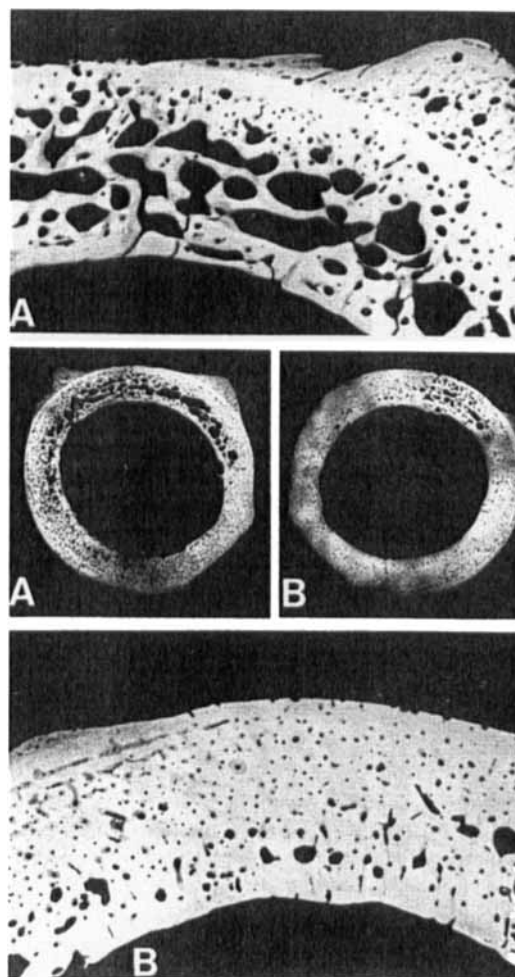


Figure 5. Paired microradiographs of bone cross-sections taken from level 4. The cis-cortex (plated surface) is closest to the top of the page. (A) Standard plated bone cross-section (2x) and enlargement of cis-cortex (6x). (B) Experimental plated bone cross-section (2x) and enlargement of the cis-cortex (6x).

Bone morphology

More porosity occurred in the standard compared with experimental plated bone (Table 1, Figure 5). Within the same implant type, the cis-cortex demonstrated greater bone porosity, and the bone porosity was larger in sections located near the plate center.

Light-microscopic data showed no difference for mean osteoid thickness between standard and experimental plated bones. Osteoid seam circumference, number of osteoid seams, and resorptive cavities per area of bone were greater in standard plated bone (Table 2). Fluorochrome microscopic data showed no difference in bone apposition rates. More fluorochrome labeling was present in standard plated bone (Table 3).

Table 1. Percent porosity of the femoral cross-sections. Standard plated and experimental plated bones (x SEM; n 10)

Level	Cortex	Plate	
		Standard	Experimental
Undecalcified sections			
1	Cis	8.4 1.8	3.6 0.9
3	Cis	11.5 2.3	4.2 1.1 ^a
Microradiographs			
4	Cis	14.4 3.5	6.2 1.7 ^a
4	Trans	4.1 1.0 ^b	2.1 0.2 ^{ab}

^a Significant difference between paired femurs (i.e., SP vs. EP bone): $P \leq 0.05$.

^b Significant difference between cis and trans-cortex of the same femur: $P \leq 0.05$.

Normal porosity for canine long bones: 1-4 percent (Harris et al. 1968).

Table 2. Light microscopic data from the cis-cortex of undemineralized sections (x SEM, n 10)

Level		Plate	
		Standard	Experimental
Osteoid seam thickness (μ)			
1		10.5 0.1	10.6 0.1
3		11.0 0.1	10.7 0.1
Osteoid seam circumference (μ)			
1		276.5 9.6	222.2 11.2 ^a
3		246.9 7.6	180.1 7.2 ^a
Osteoid seams/mm ²			
1		1.8 0.2	1.0 0.2 ^a
3		2.2 0.3	1.6 0.2 ^a
Resorptive cavities/mm ²			
1		1.3 0.2	0.8 0.1 ^a
3		2.5 0.2	1.2 0.2 ^a

^a Significant difference between femur pairs: $P \leq 0.05$.

Table 3. Fluorescence microscopy data from the cis-cortex of undemineralized sections (X SEM, n 10)

Level		Plate	
		Standard	Experimental
Appositional rate (μ /day)			
1		1.27 0.01	1.27 0.01
3		1.21 0.03	1.26 0.02
Percent fluochrome-labeled osteons			
1		16.9 2.2	7.2 1.9 ^a
3		18.3 2.0	10.3 2.6 ^a

^a Significant difference between femur pairs: $P \leq 0.05$.

Bone cross-sections at levels 3 and 4 showed no differences between implant types for bone cortical thickness, medullary canal area, and cross-sectional area. The cis- and trans-cortex width averaged 2.6 mm, the bone area 1.2 cm², and the medullary canal 1.1 cm².

Discussion

The plate-bone interface mechanics are complex, and the relationship between screw tightness and overall composite rigidity of the plate-bone system are not fully characterized. Mechanical tests and finite element analysis indicate that slipping occurs between the conventional plate and bone (Beaupré et al. 1988). Loosening the bone screws increases plate-bone slippage and reduces composite rigidity (Carter et al. 1984), whereas increasing the bond between plate and bone through the use of porous-coated implants increases composite rigidity and induces greater bone loss (Pilliar et al. 1979). The plate-bone interface, therefore, affects final composite rigidity of the bone plate system and directly affects bone mass.

In our experiment, silicon elastomer was chosen because it can withstand the compression between plate and bone without immediate plastic deformation, is biocompatible (Brown et al. 1977, Buchhan et al. 1982), and it exhibits a small plastic-deformation over time (i.e., 15 percent and 18 percent compression set after 6 months and 1.5 years at room temperature (Dow Corning 1972)). In our experimental plated bone, screw callus was distributed among all the screw tracts, but in standard plated bone, screw callus was seen predominantly in the screw tracts at the ends of the plate. We equate screw callus to loading of screws due to load transfer between plate and bone. The callus pattern in experimental plated bone matches the screw load pattern, determined by Cheal (1983) using finite element analysis of a plate-bone model that allows motion at the interface. They found that the forces on all the screws are nearly equal. This contrasts with the standard plated bone, where screw callus is predominantly located among the outer screw tracts. It matches the screw tract callus pattern seen in other in vivo plating experiments (Strömberg et al. 1978; Carter et al. 1984). Cheal's finite element analysis of a direct contact plate-bone model, which does not allow slippage, shows forces are greatest on outer screws. Load transfer to the plate occurs abruptly at the plate ends through the end screws. Hence, the screw callus distribution illustrates the differences in the strain pattern and the transfer of load in the standard and experimental plates.

Another factor in reducing bone loss is the contact pressure. High plate-bone forces produce areas of ischemia and promote bone remodeling under the plate (Gunst 1980). A reduction in this contact pressure should preserve bone mass. The lower plate-bone contact pressure seen in the experimental plate translates into less bone loss *in vivo*.

Breakage of the Silastic® was an unexpected finding in a situation where no instability exists. Cyclic loads from weight-bearing activity, shear forces between the plate and bone, in addition to the compressive static load from the plate probably contributed to the failure of the Silastic®. This failure is expected to reduce the composite rigidity of the bone plate system. More tear-resistant forms of Silastic® are available and would eliminate this problem. Breakage of the Silastic® is also undesirable because it would release Silastic® particles into the tissue. Chronic Silastic® implantation has

been associated with foreign-body reactions (Swanson et al. 1984), although it was not noted in this study.

Two other research groups have tried viscoelastic material with compression plates. Both groups used ultra high molecular weight polyethylene (UHMWPE) in canine femoral osteotomy models. One group placed the UHMWPE under the plate, whereas the other group placed the UHMWPE between the screw heads and the plate (Daniels et al. 1985; Park-Joon et al. 1987). Less bone loss and greater bone strength were seen in femurs plated with the modified plates as compared with conventional plates.

These results, as well as our own results, suggest that modifying the bone-plate interface with viscoelastic material will reduce bone loss. Refinement in this design concept and additional investigations are necessary before clinical implementation is possible.

References

- Akeson WH, Woo SL, Rutherford L, Coutts RD, Gonsalves M, Amiel D. The effects of rigidity of internal fixation plates on long bone remodeling. A biomechanical and quantitative histological study. *Acta Orthop Scand* 1976; 47(3):241-9.
- Beaupré G S, Carter D R, Orr T E, Csongradi J. Stresses in plated long bones: the role of screw tightness and interface slipping (published erratum appears in *J Orthop Res* 1988;6(3):466). *J Orthop Res* 1988;6(1):39-50.
- Brown S A, Merritt K, Mayor M B. Considerations of allergy and mechanics in the selection of orthopaedic implant materials (Abstract). *Bull Hosp Joint Dis* 1977;38(2): 67-8.
- Buchhan GH, Willert HG. Effects of plastic wear particles on tissue. In: *Biocompatibility of Orthopedic Implants* (Ed. Williams D F). CRC Press, Boca Raton 1982;1:249-68.
- Carter D R, Shimaoka E E, Harris W H, Gates E I, Caler W E, McCarthy J C. Changes in long bone structural properties during the first 8 weeks of plate implantation. *J Orthop Res* 1984;2(1):80-9.
- Cheal E J, Hayes W C, White A A. Stress analysis of a simplified compression plate fixation system for fractured bones. *Comput Struct* 1983;17(5-6):845-55.
- Conlogue G J, Marcinowski F 3d. Microradiography: a theoretical basis and practical applications. *Radiol Technol* 1987;58(4):301-9.
- Daniels A V, Cone L L, Kenner G H, Schultz R S. The polymeric underplate: Canine implant study. *Transactions of the 31st Annual ORS Meeting* 1985;10:164.
- Designing with Silastic® Silicone Rubber. *Bulletin, Dow Corning Corp* 1972;17:158.
- Gunst M A. Interference with bone blood supply through plating of intact bone. In: *Current Concepts of Internal Fixation of Fractures* (Ed. Uthoff H K). Springer Verlag, Berlin 1980:268-76.
- Harris WH, Haywood E A, Lavorgna J, Hamblen D L. Spatial and temporal variations in cortical bone formation in dogs. *J Bone Joint Surg (Am)* 1968;50:1118-28.
- Läftman P, Sigurdsson F, Strömberg L. Recovery of diaphyseal bone strength after rigid internal plate fixation. An experimental study in the rabbit. *Acta Orthop Scand* 1980;51(2):215-22.
- Park-Joon B U, Kuo R F, Rim K, Choi W W. Washers found to decrease plate stress shielding. (Abstract). 13th Annual Meeting of the Society for Biomaterials, 1987.
- Pilliar R M, Cameron H U, Binnington A G, Szivek J, Macnab I. Bone ingrowth and stress shielding with a porous surface coated fracture fixation plate. *J Biomed Mater Res* 1979; 13(5):799-810.
- Schatzker J, Sumner Smith G, Clark R, McBroom R. Strain gauge analysis of bone response to internal fixation. *Clin Orthop* 1978;(132):244-51.
- Strömberg L, Dalén N. Atrophy of cortical bone caused by rigid internal fixation plates. An experimental study in the dog. *Acta Orthop Scand* 1978;49(5):448-56.
- Swanson A B, Nalbandian R M, Zmugg T J, Williams D, Jaeger S, Maupin B K, Swanson G D. Silicone implants in dogs. A ten year histopathologic study. *Clin Orthop* 1984;(184):293-301.
- Uthoff H K, Dubuc F L. Bone structure changes in the dog under rigid internal fixation. *Clin Orthop* 1971;81:165-70.
- Uthoff H K, Finnegan M. The effects of metal plates on post-traumatic remodelling and bone mass. *J Bone Joint Surg (Br)* 1983;65(1):66-71.